


Article

Some Investigations on a Possible Relationship between Ground Deformation and Seismic Activity at Campi Flegrei and Ischia Volcanic Areas (Southern Italy)

Ciro Ricco ¹, Simona Petrosino ¹, Ida Aquino ^{1,*}, Carlo Del Gaudio ¹ and Mariarosaria Falanga ² 

¹ Istituto Nazionale di Geofisica e Vulcanologia, Sezione di Napoli—Osservatorio Vesuviano, 80124 Naples, Italy; ciro.ricco@ingv.it (C.R.); simona.petrosino@ingv.it (S.P.); carlo.delgaudio@ingv.it (C.D.G.)

² Dipartimento di Ingegneria dell'Informazione ed Elettrica e Matematica applicata/DIEM, Università degli Studi di Salerno, 84084 Fisciano, Italy; mfalanga@unisa.it

* Correspondence: ida.aquino@ingv.it; Tel.: +39-081-6108-337

Received: 19 March 2019; Accepted: 8 May 2019; Published: 15 May 2019



Abstract: In the present paper, we analyse ground tilt and seismicity at Campi Flegrei caldera and Ischia Island, two volcanic areas located in the south of Italy. These areas have been well studied for many years from a petrological, volcanological and geophysical view point. Moreover, due to the high seismic and volcanic risk for the populations living there, they are continuously monitored by networks of geophysical and geochemical sensors. We summarize the most important results that we obtained so far, concerning the observations of relationships between seismic activity and ground tilt anomalies, focusing on the time interval 2015–2018. First, we present a detailed description of the tiltmeter and seismic networks in both the investigated areas, as well as their development and improvement over time that has enabled high quality data collection. From the joint analysis of the seismic and borehole tiltmeter signals, we often notice concurrence between tilt pattern variations and the occurrence of seismicity. Moreover, the major tilt anomalies appear to be linked with the rate and energy of volcano-tectonic earthquakes, as well as with exogenous phenomena like solid Earth tides and hydrological cycles. The analysis that we present has potential applicability to other volcanic systems. Our findings show how the joint use tilt and seismic data can contribute to better understanding of the dynamics of volcanoes.

Keywords: ground deformation; seismic phenomena; Campi Flegrei Caldera; Ischia Island; volcanic risk; seismic and tiltmeter networks; ground tilt anomalies

1. Introduction

A multidisciplinary analysis of data coming from different fields, such as tilt and seismic observations, represents a successful strategy to investigate the dynamics of volcanoes. Ground deformation related to fracture processes or induced by fluid mass movements are often associated with the occurrence of seismicity, and the two phenomena can be interpreted in a unified framework. For example, joint investigation of tilt and seismic data has revealed inflation-deflation cycles associated with gas recharge and discharge in volcano conduit or with magma pressurization at shallow depths, as has been found at Stromboli [1] and Montserrat [2], respectively. The hypothesis of a shallow source associated with a steam-filled crack has also been proposed at Mount St. Helen [3], on the basis of the correlation between ground tilt and local seismicity. Tilt offsets have clearly been observed concurrent with seismic swarms, as in the case of Etna where the offset associated with the seismic swarm on January 2001 indicated the occurrence of both seismic and aseismic deformation mechanisms related to a fluid-driven faulting episode [4]. A strong reversal of the tilt direction was also

detected at Vesuvius between the end of 2000 and the first months of 2001 and it was likely related to the consistent reduction of the energy released by local earthquakes, after the strong seismic crises that affected the volcano in late 1999–2000 [5]. Continuous and high resolution tilt measurements are crucial for monitoring purposes. Precursory phenomena of volcanic eruptions, like ground deformations induced by the ascent of magma can often be small and difficult to detect. As a result, monitoring instruments and surveying techniques that have sub-centimetric accuracy must be used [4]. The tilt data correlated with seismic, explosive and pyroclastic activity have been even used to forecast times of increased volcanic hazard [2].

The assessment of the seismic and volcanic risk is particularly relevant in densely populated areas. The volcanoes of the Neapolitan District (Campi Flegrei, Vesuvius and Ischia) are considered among the most dangerous in the world; the risk being very high because it is strongly urbanized and also includes an impressive historical, artistic and cultural heritage. Numerous studies (see Section 2 and references therein) have been conducted on these volcanoes to model their dynamics and improve eruption forecasts.

Due to a necessity to improve the monitoring system, the geodetic and seismic networks have undergone several technical upgrades throughout the years, thus allowing reliable joint analysis of ground tilt and seismicity. The study of ground deformation in the Campanian volcanic area during the past 20 years has been carried out by using surface tiltmeters that are accurately installed in isolated locations protected from strong environmental factors [6,7]. A great development in the last 5 years has taken place with the use of tilt sensors in deep holes [8]. Similarly, from a seismological view point, there has also been a significant increase over time in both the density and the quality of the instruments, improving the network performance [9,10]. The progressive upgrade of the seismic network has been paralleled by the development of more accurate analysis techniques [9,11–14].

In this paper, we analyse data recorded by the tiltmeter and seismic networks operating at Campi Flegrei, with the aim of providing a further contribution to the understanding of the link between ground deformation and seismic activity. In particular, we focus on the 2015–2018 interval, due to the availability of high quality data from new borehole tiltmeters (Figure 1). A similar investigation is also carried out at Ischia Island. From the joint analysis of tilt and seismic data, we find evidence of relationships between tilt patterns and the rate and energy of volcano-tectonic earthquakes. Moreover, we identify tilt anomalies related to both high energy seismic swarms and to external sources such as Earth tidal and hydrological cycles. These relationships suggest that the observed ground deformation trend is the result of a complex superposition of the endogenous dynamics and exogenous processes.

2. Geological and Geophysical Background

The Phlegraean Volcanic District is one of the most hazardous volcanic areas in the world, consisting of the Campi Flegrei caldera, the volcanic islands of Ischia and Procida, and a number of submerged vents, aligned in the NE-SW direction [15–21] (Figure 1b). The Phlegraean Volcanic District originated following the Pliocene-Quaternary extension, which generated the graben of the Campanian Plain between the western sector of the Appenine Chain and the eastern margin of the Tyrrhenian Sea. It is composed mostly of monogenetic centers, with fissure-type magmatic systems [19–23].

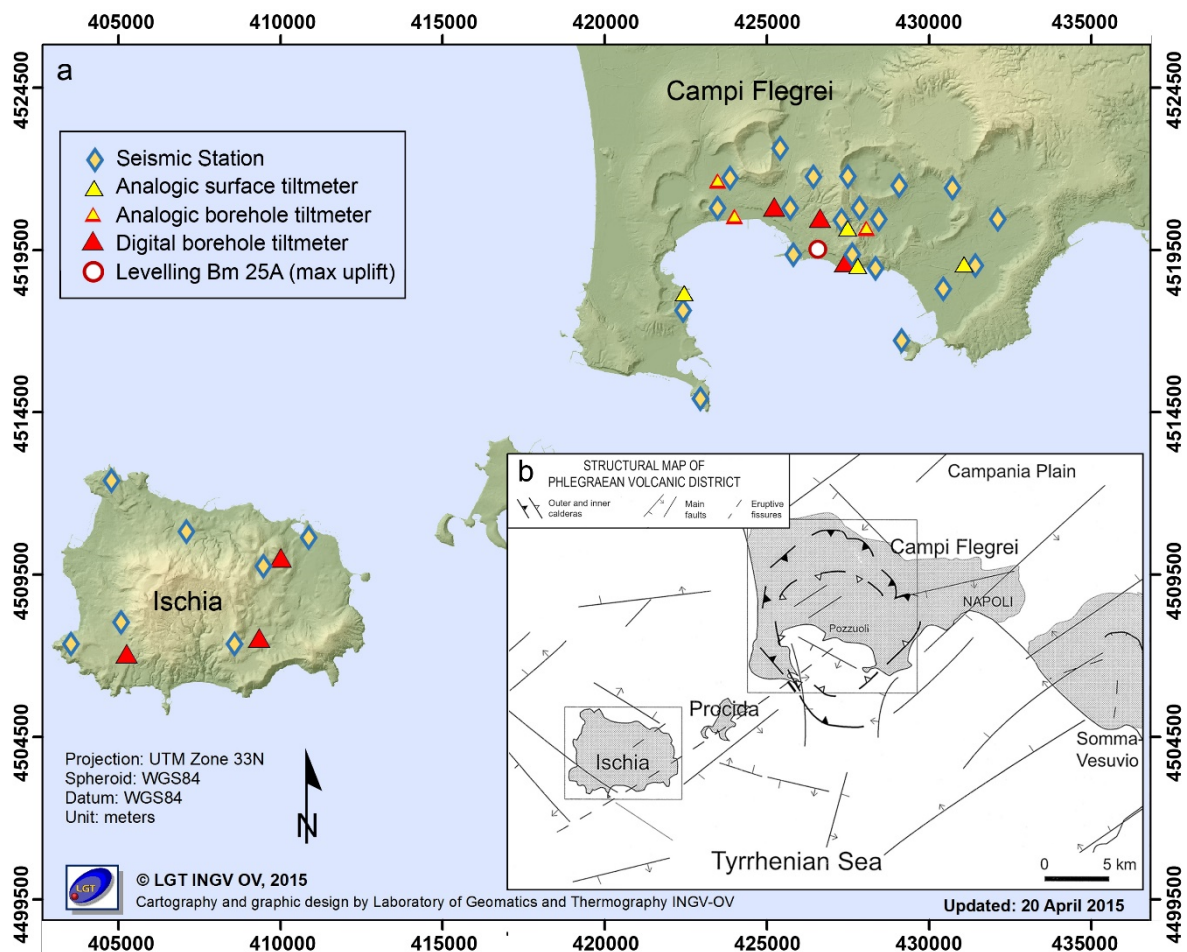


Figure 1. (a) Tiltmeter (triangles) and seismic (diamonds) network for ground monitoring at Campi Flegrei and Ischia Island. The inset (b) shows the Geological and Structural map of the Phlegraean Volcanic District, modified from [20].

2.1. Campi Flegrei

The Campi Flegrei caldera is commonly considered one of the most dangerous active volcanic systems on Earth, extending into a densely inhabited metropolitan region on the western edge of Napoli bay (Southern Italy). In fact, the western suburbs of the city of Naples lie within the caldera rim and the town of Pozzuoli is completely situated within the caldera; a possible explosive eruption could directly impact more than 1 million people. This caldera covers an area of approximately 200 km² defined by a quasi-circular depression, half onland, half offshore [24]. It is a resurgent structure generated by two major collapses, the Campanian Ignimbrite (~39 ky), with an erupted volume of products ranging between 100 and 200 km³ [25] and the Neapolitan Yellow Tuff with 20–50 km³ of erupted products (~15 ky) [15,26]. Post-caldera volcanic activity has been confined within the caldera and characterized by more than 60 eruptions, mostly explosive and some effusive [15]. The last eruption occurred in 1538 with the formation of a scoria cone called Monte Nuovo. Preceding the eruption a ground uplift occurred in the central area of the caldera, accompanied by intense seismic activity [21,27,28].

After the Monte Nuovo eruption, Campi Flegrei has shown a complex deformation history; indeed, ground deformation exhibited a downward trend until the middle of the last century. Over the last 2 millennia, an accurate reconstruction of vertical ground movements has been performed through many studies [28–32]. The bradyseism consists of a slow subsidence alternating with fast ground uplifts that are often accompanied by seismicity. In more recent times, three major and several minor uplift episodes have occurred. The first bradyseismic crisis occurred between 1950 and 1952 with a maximum uplift of 80 cm, during which the population did not detect any earthquakes [31]. In the

periods 1969–1972 and 1982–1984, two important episodes of inflation occurred, accompanied by seismic crises. These episodes produced maximum uplifts of 177 and 179 cm, respectively, centered on the town of Pozzuoli (Figure 2). The geometrical shape of the deformation remained constant in time. It had a circular symmetry around Pozzuoli and regularly decreased towards the margin of the caldera [33–36]. Both the 1969–1972 and 1982–1984 uplifts have been attributed to a magmatic intrusion [32]. After 1984, minor deformation episodes occurred in 1989, 1994 and 2000. Starting from 2005, a new ground uplift began. This uplift has different characteristics in fact, the rate of deformation since 2005 is about 20 times slower compared to the 1969–1972 and 1982–1984 episodes. The last lifting phase began in 2012 and is still ongoing [31] (Figure 2). The two recent uplift phases were accompanied by seismic activity both with Long Period (LP) and Volcano-Tectonic (VT) earthquakes [37].

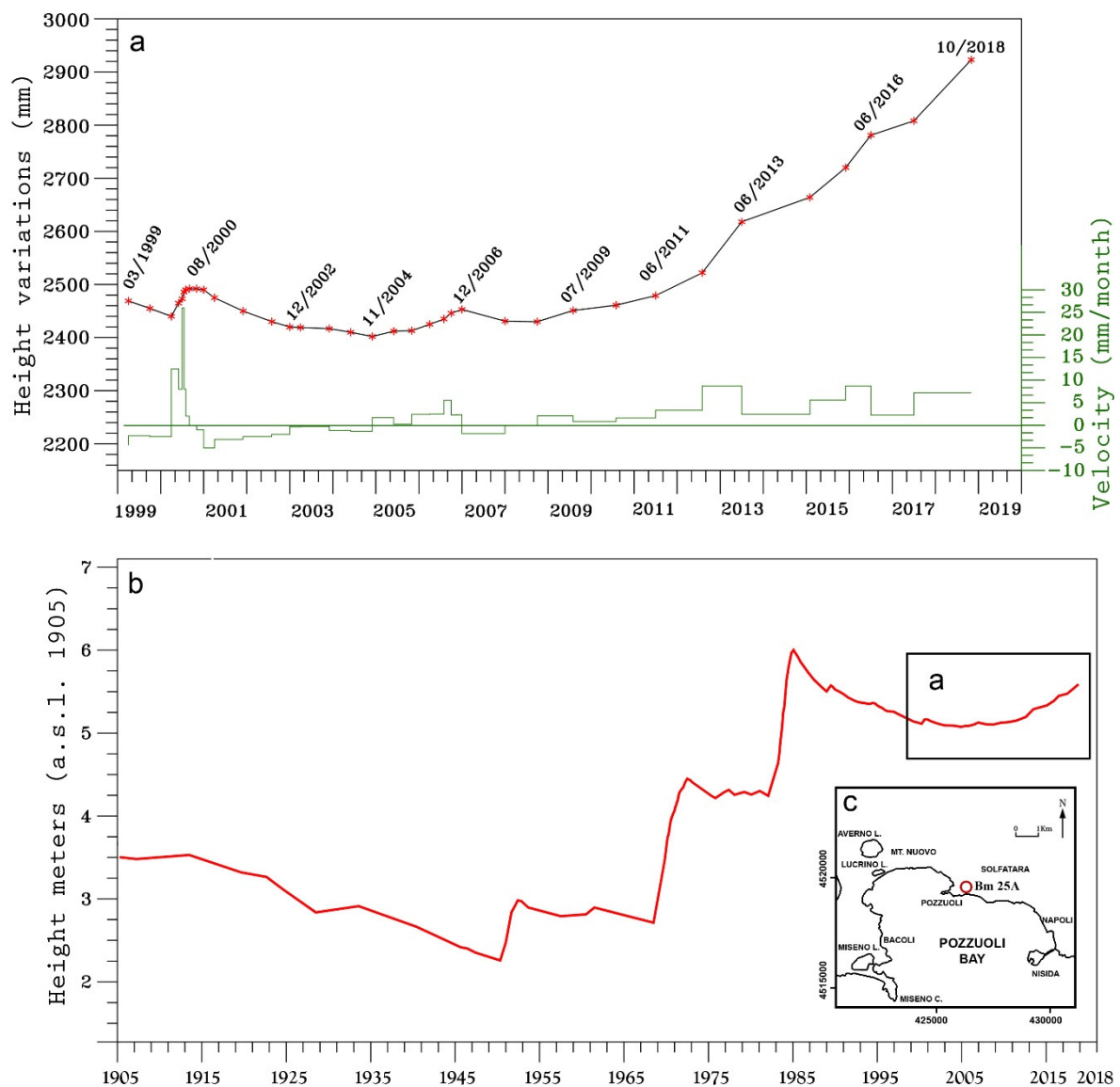


Figure 2. (a) Height variation of the benchmark 25A (Bm 25A) which records the maximum vertical displacement in the Campi Flegrei area in the last twenty years; the ground uplift rate in mm/month are shown in green. (b) Height variations observed from 1905 to 2018 ([31] modified and supplemented with data from leveling surveys carried out after 2009). (c) Schematic map with the Bm 25A location (red circle) coincident with the maximum uplift measured.

The most remarkable LP sequence started on 23 October 2006 [37] and lasted about seven days. During the three days of climax (26–28 October 2006), more than 300 events occurred, located at depths

of about 500 m b.s.l. beneath the Solfatara crater. Their source mechanism was ascribable to the acoustic resonance of a crack filled by a water-gas mixture of hydrothermal origin [38–41]. Two minor LP episodes were observed in January 2008 and June 2010 [42]. The VT activity shows a periodic occurrence, alternating intense swarms lasting a few hours or even minutes, and phases of very low seismicity rate [43]. Major seismic swarms composed of up to 200 earthquakes with duration magnitude M_d up to 2.5, were observed in October 2005, October 2006, January 2008, March 2010, September 2012, March 2014, October 2015, July 2016, August 2016, March 2018, September 2018 and October 2018 [13,14,42,43]. The most energetic earthquakes since the recent uplift phase occurred in October 2015 ($M_d = 2.5$), July 2016 ($M_d = 2.1$), March 2018 ($M_d = 2.4$), September 2018 ($M_d = 2.5$) and October 2018 ($M_d = 2.0$). The earthquakes were generally located beneath the Solfatara-Pozzuoli area, at depths up to 4 km b.s.l. [37,42]. The waveforms and spectral features of the VTs are indicative of a source process involving brittle shear failure, possibly induced by the pressurization of the hydrothermal system and fluid flow towards the surface [37,44].

2.2. Ischia Island

The volcanic island of Ischia is located in the westernmost portion of the Phlegraean Volcanic District (Figure 1b) and represents the subaerial portion of a volcanic field, whose activity started around 150 ky [45]. It is located on the Tyrrhenian border of central Italy, at the intersection of regional fault systems, with NW-SE (Appennine) and NE-SW (anti-Appennine) trends [19–23]. Ischia island rises over 1000 m above the seabed [46] and covers an area of 46.4 km², it is morphologically dominated by Mt Epomeo (787 m above sea level), located in a central sector of the island along the NE-SW alignment of Mt Vezzi and Mt Cotto in the SE sector. The coast is characterized by steep cliffs and some less steep slopes that plunge into the sea [19,47–50]. The volcanic activity started around 150 ky and was characterized by several effusive and explosive eruptions alternating with periods of quiescence [23,46–48]. The most impacting event on the island is the caldera forming eruption of the Green Tuff of Mt Epomeo, which occurred 55 ky and caused the collapse of the central sector of the island, followed by resurgence of the Mt Epomeo block starting from 30 ky [23,48–50]. The last eruption occurred in 1302 A.D. with the effusive eruption of Arso, located in the eastern sector of the island [23,51,52].

Ischia is characterized by significant ground deformation, whose first quantitative measurement was made in 1913 by the Italian Army Geographic Institute (IGM) through a precision leveling survey and repeated in 1967 by the Italian Geodetic Society (SGI). From 1978 to 2010, new leveling lines including new benchmarks were installed by the Istituto Nazionale di Geofisica e Vulcanologia–Osservatorio Vesuviano (INGV–OV) and numerous surveys have since been carried out, the latest of which was carried out in November 2017. Starting from 1996, a network involving 17 Global Positioning System (GPS) stations has been set up on the island [53]. At the same time, the in-situ ground deformation monitoring of the island has been further expanded using the Differential Synthetic Aperture Radar Interferometry (DInSAR) technique [54]. All measurements made along the geodetic network of the island of Ischia clearly show a persistent and significant subsidence, which can be observed in particular in the central-southern and north-western sectors of the island with movements of the order of 1 cm/year [55,56]. The results obtained from the high precision leveling survey carried out in November 2017 in the northwestern area of the island identify a localized and pronounced anomaly of ground deformation in the epicentral area of the recent M_d 4.0 earthquake, which occurred on 21 August 2017 [8].

The seismicity of the island is mainly located in the northern sector and it is related to the resurgent block of Mt Epomeo. In the past, the activity was intense: strongest historical earthquakes ($VIII < I < XI$ MCS) occurred in the eighteenth and nineteenth centuries [57,58]. We recall the destructive earthquakes of March 4, 1881 ($I = IX$ MCS, [59,60]) and 28 July 1883 ($I_{max} = XI$ MCS and $M = 5.2$, [57,60]).

Recent seismicity of Ischia consists of low-magnitude earthquakes, most part of them located at depths shallower than 2 km [10]. In 2017, on August 21 an earthquake of $M_d = 4.0$ (moment magnitude

Mw = 3.9) occurred, causing severe damage in the area of Casamicciola. This event (hereafter referred to as EQ2017) was located at about 1.2 km b.s.l. and it was followed by a seismic sequence of about 30 earthquakes. Since that date, the rate of seismicity has remained low. The last relevant sequence occurred in November 2018 and consisted of 20 earthquakes with maximum Md of 0.7.

3. Tilt and Seismic Measurements: Data Analysis and Results

3.1. Campi Flegrei

The tiltmeter network for the monitoring of ground deformation induced by phlegraean bradyseism has a long history dating back to 1985 [6,7]. In 2006, the tiltmeter network consisted of five analog surface tiltmeters and two analog borehole tiltmeters installed at 7 and 5 m depth but later, from 2006 to 2011, three more surface stations were installed in locations of low background noise. In 2013, another analog borehole tiltmeter close to Pisciarelli fumarole field (near Solfatara) at 1.5 m depth was installed. Finally, in 2015, three borehole stations equipped with digital sensors of the model “Lily Self-Leveling Borehole Tiltmeter” were installed into 25 m deep wells [61,62] (Figure 1). The stainless steel instruments have a cylindrical shape with dimensions of 51 × 915 mm. At the bottom, an electrolyte bubble and temperature sensors, and a magnetic compass (to detect the change of magnetic declination, counter clockwise from N), are positioned. The sensing device is a self-levelling sensor on a range of ± 10 degrees, with a dynamic range of ± 330 μ radians and a resolution less than 5 nradians [63]. Ground tilt variations are measured along two orthogonal directions NS and EW; they are recorded with a sampling rate of 1 sample (defined as the average of 8000 readings) per minute.

The seismic network managed by the INGV–OV is composed of both permanent installations and mobile deployments (Figure 1). Since 2005 the seismic network has undergone to several technological improvements. The analog permanent stations are equipped with short-period 1 Hz seismometers (Mark L4C, 1 Hz Lennartz LE-3Dlite, Geotech S13); the digital dataloggers are coupled with three-component broadband seismometers (Guralp CMG40T, Guralp 3TB/5TB, Trillium 120 P). The signals are continuously recorded at 100 sps and telemetered to the acquisition centre. The mobile network consists of stand-alone dataloggers with both 1 Hz (Lennartz LE-3Dlite) and three-component broadband sensors (Lennartz LE3D/20s, Geotech KS2000, Guralp CMG-40T). The data are sampled at the rates of 125 Hz or 100 Hz. The updated configuration of the seismic network is reported at the URL www.ov.ingv.it and further details can be found in [9].

From historical observations, leveling surveys, GPS and DInSar measurements, the centroid of the deformation field is permanently located in Pozzuoli [42,53,54]. The radially of the observed deformation constitutes a first-order effect due to the phases of ground uplift and deflation. However, epochs in which the angular component of the strain undergoes sharp changes over time are superimposed to the general trend. These variations, here called tilt reversal, are recorded only by tiltmeters that measure the non-diagonal components ($i \neq j$) of the deformation tensor (pure tilt in a solid halfspace) [64].

Since 2015, the three borehole instruments (CMP, ECO and HDM) for which the background noise is greatly reduced, provides time series that are easier to interpret than the superficial ones. For these tiltmeters, the inclination detected by the NS components have always been consistent with the deformation recorded by the vertical component of the GPS stations located nearby. In addition, the resulting tilt vector obtained from the composition of the NS and EW component, provides directions of ground inclination generally congruent with those obtained from the deformation field induced by uplift of Pozzuoli only for CMP and HDM (located respectively at NNW and ESE of Pozzuoli). Conversely, the ECO station, located NE of Pozzuoli, tilted in line with the uplift only from March 2017 to July 2018; before this time interval its tilting direction was NW and then W.

Based on the clear symmetry of the tilt pattern at ECO station, we identified on the hodograph the points where there is an abrupt switch in tilting direction (Figure 3).

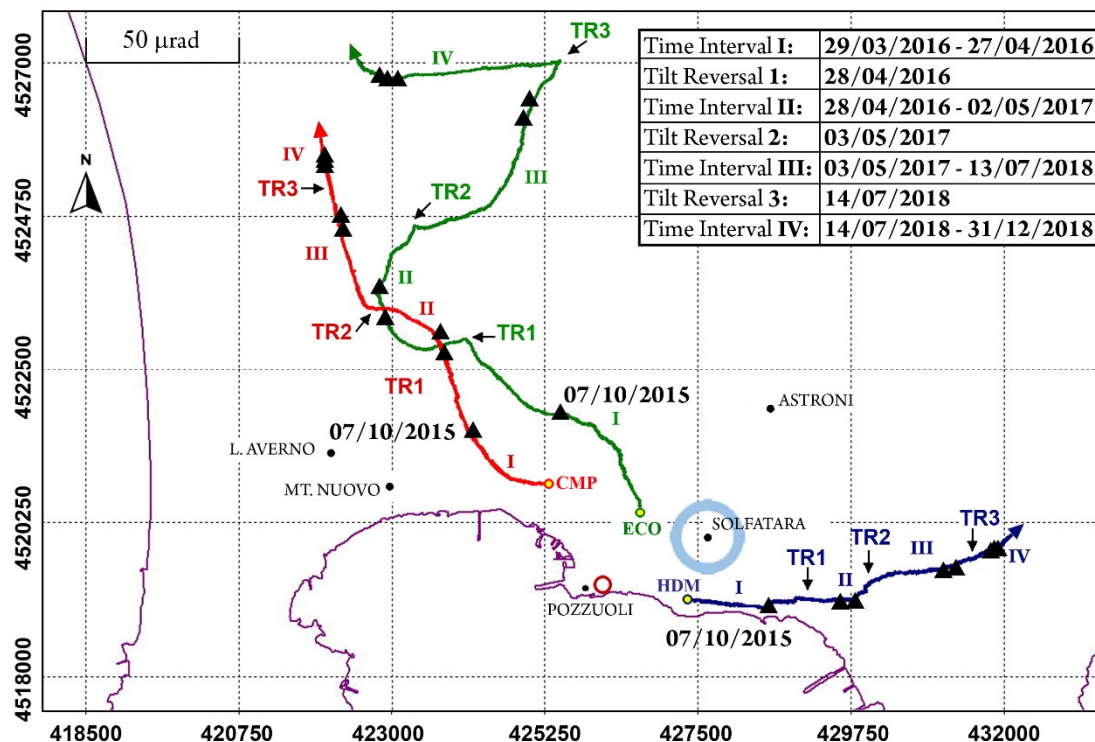


Figure 3. Schematic map of Campi Flegrei, superimposed on a grid representing the two-dimensional plane of ground inclinations, in which each mesh is equivalent to a tilt variation of $50 \mu\text{rad}$. The three sites CMP, ECO and HDM are distinguished by different colors (red, green and blue, respectively), as well as the curves that originate from them: the latter indicates the cumulative tilt variation (hodograph) recorded since 29 March 2015 to 31 December 2018. The roman numerals indicate four time subintervals separated by the occurrence of a tilt reversal episode (TR) and characterized by different kinematics. On the same grid the earthquakes with $M_d > 1.6$ are shown with black triangles and the area of maximum uplift is shown with a red circle. The light blue circle encompasses the area where VT seismicity occurred.

These points mark the sub-division into four time intervals that seem to be characterized by a geometric similarity in response to distinct kinematics:

Time Interval I: 29 March 2016–27 April 2016

During this time (Figures 3 and 4), the tilting direction at CMP and HDM is perfectly compatible with that induced by the ground uplift centered at Pozzuoli, while at ECO it is strongly polarized to the NW. Tilting directions show a concave and convex trend respectively at CMP and ECO while HDM is almost straight.

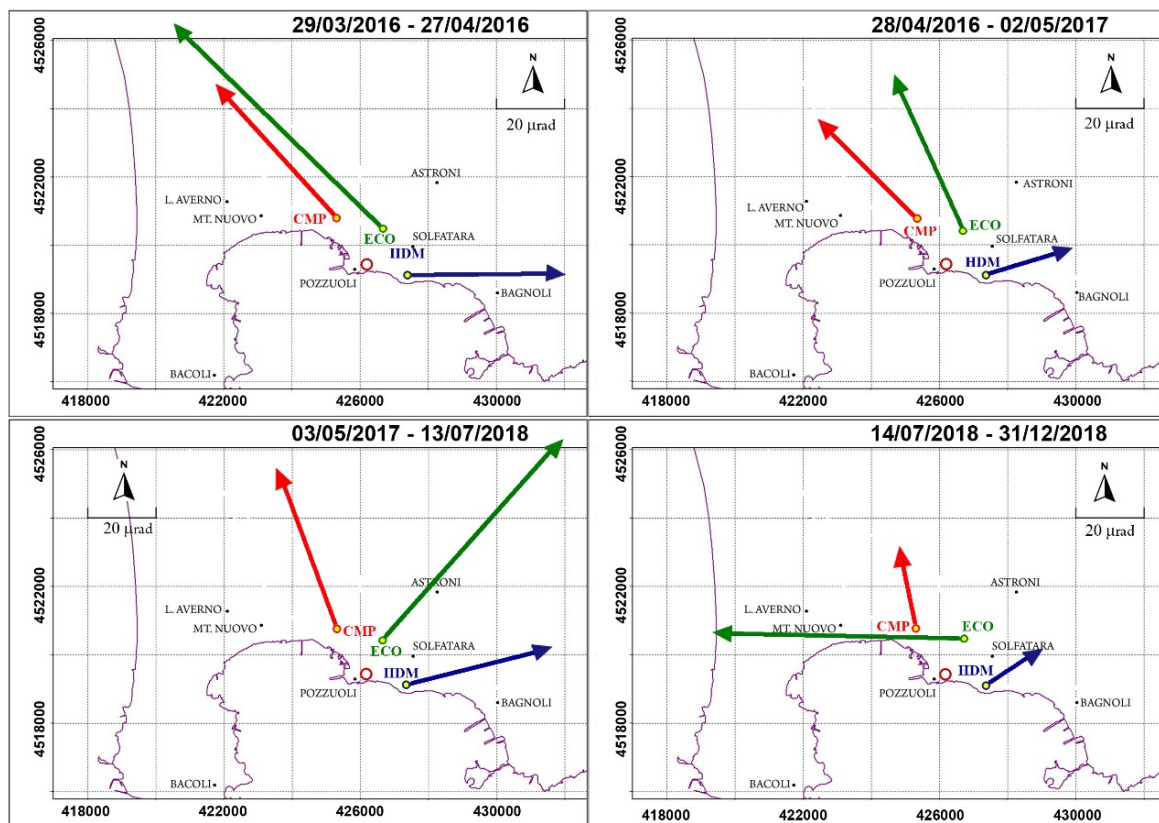


Figure 4. Tilt direction patterns observed at each borehole station during the four Time Intervals discussed in the text and showed in Figure 3. Tilt vectors point outwards from the area of maximum uplift (shown with a red circle).

On 7 October 2015, just before the seismic swarm, an evident tilt anomaly on the signals acquired by the ECO station was observed; in particular, the EW component of the borehole digital tiltmeter recorded four distinct offsets ranging between 0.5 and 2.8 μ rad before four out of the six most energetic VTs. In addition, a constant delay of 9 minutes between the negative and/or positive offsets and the occurrence of the seismic events was surprisingly observed, while the NS component of HDM always showed peaks on the signal 1 minute before. The offset and peak amplitudes do not depend on the earthquake magnitude. The pre-seismic deformation recorded by ECO was permanent, i.e., the site tilted about 5 μ rad W and did not recover this deformation (Figure 5).

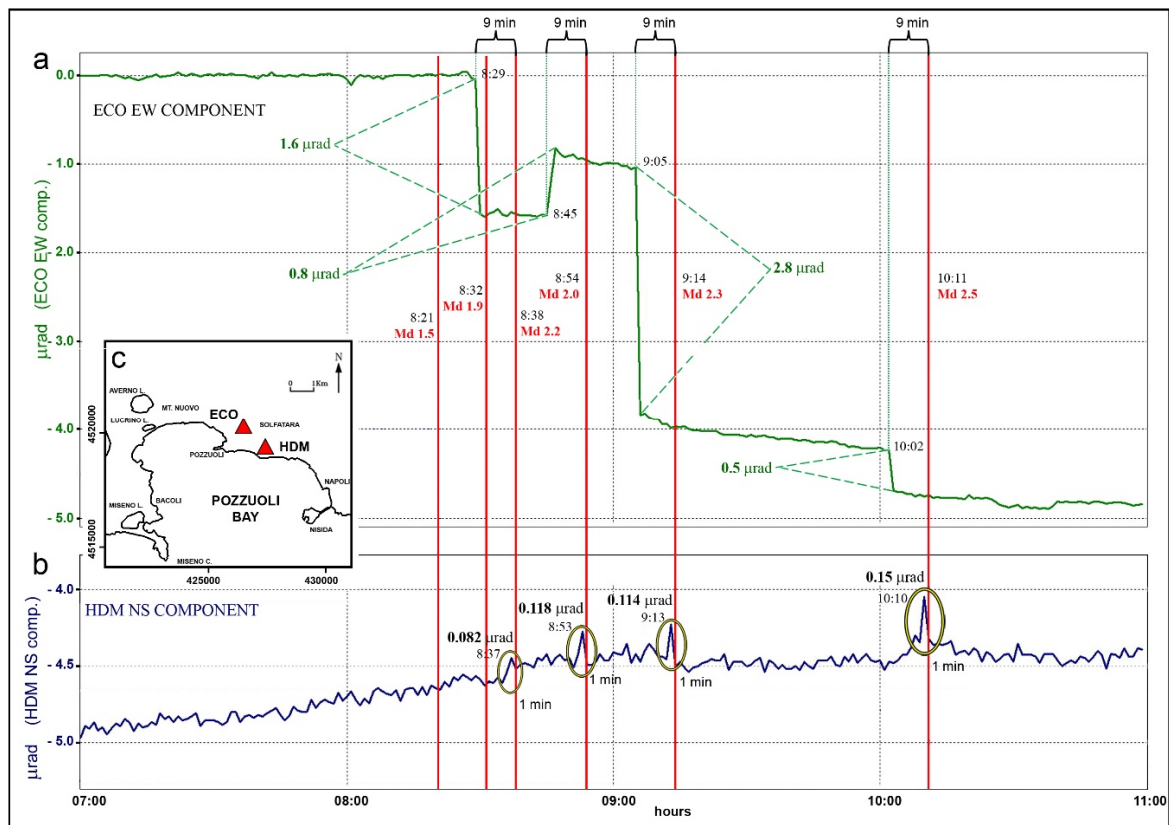


Figure 5. Detailed analysis of the 4-hour long time series recorded before and after the earthquakes of October 7, 2015 observed at (a) ECO (EW component in green) and (b) HDM (NS component in blue). The EW component recorded four distinct offsets ranging between 0.5 and 2.8 $\mu\text{radians}$ 9 minutes before the four most energetic VTs (red vertical lines); instead the NS component of HDM always showed peaks on the signal 1 minute before the VT. (c) Location of the ECO and HDM tilt stations.

Time Interval II: 28 April 2016–2 May 2017

The interval (Figures 3 and 4) starts with a strong tilting reversal (TR1) affecting both components of ECO. This epoch is characterized by kinematics where, at CMP and HDM sites the deformation is consistent with the uplift whereas, after the reversal, ECO follows a NNW tilting direction. Differently from the previous time interval it is further noted that the tilt recorded at CMP and ECO shows opposite concavities.

Time Interval III: 03 May 2017–13 July 2018

Also in this case (Figures 3 and 4), the epoch begins after a tilt reversal episode (TR2) with a perfect correspondence between the deformation field generated by lifting of the ground and tilt response. The tilt at the three sites radiate outwards from the site of maximum deformation, and paths of CMP and HDM are unusually straight while ECO shows a concave trajectory.

Time Interval IV: 14 July 2018–31 December 2018

The ECO tilt pattern (Figures 3 and 4) changes completely (TR3 episode) from July 14 because its direction rotates counterclockwise from NNE to W by more than 90 degrees while CMP and HDM keep their centripetal trajectory in the same radial direction. About one and a half months later, the tilt at the ECO site reaches the maximum stretching towards the W. Similarly to TR1 and TR2, TR3 also occurs aseismically.

Before 2015, when borehole tiltmeters had yet to be installed, at least two phenomena of tilt reversal, were also recorded by surface sensors. In late July 2006 at OLB station, a reversal corresponding to a great change in the pattern and intensity of the tilt, preceded the seismicity recorded in September and October of the same year [7] (Figure 6a). This change takes place during an increase of the ground

uplift rate (from 1.7 to 5 mm/month) measured by leveling surveys (Figure 2a). In 2010, the same tiltmeter recorded another variation of the tilt pattern four days before the seismic swarm of March 30. The anomaly consisted of a reversal followed by a persistence, from 26 to 30 March, of ground tilt in the WNW direction (Figure 6b).

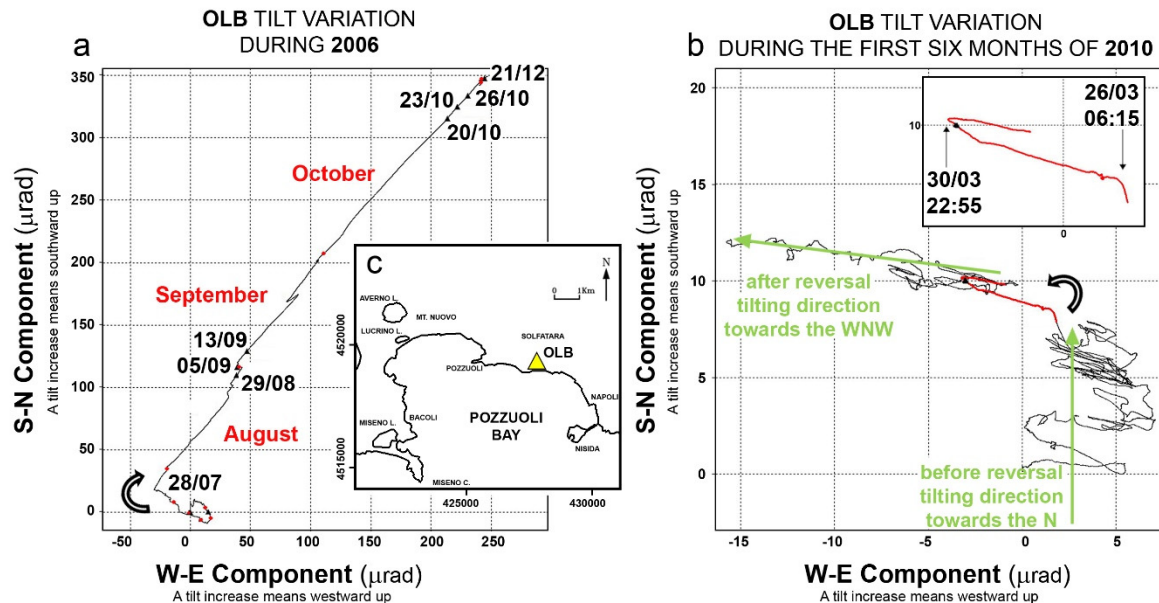


Figure 6. Plots of the tilt vector recorded at OLB before two seismic swarms. (a) The tilt reversal observed in late July 2006, indicated with a semicircular right arrow, takes place before the seismic events of September and October of the same year. (b) The tilt reversal recorded on 26 March 2010 indicated in red with a semicircular left arrow, occurs four days before the seismic swarm of late March of the same year and interrupts the tilting towards the N, forcing it towards the W. The inset shows the zoom of the tilt reversal and the arrows placed on the hodograph show the direction of ground tilting. (c) Location of the OLB tilt station.

The previous results indicate that tilt variations may occur either associated with seismicity or aseismically. This observation lead us to consider other possible causes (besides the seismic activity) that can potentially be related to tilt anomalies. In particular, the effects of the tidal forces on the ground tilt will be analysed in the next subsection.

Tidal Analysis of the Ground Tilt

The kinematic analysis of the ground tilt has evidenced the existence of peculiar features at medium/long time scales. In order to get more insight into these patterns, the time series were narrow-band filtered around the typical periods of the monthly (Mm) and fortnightly (Mf) tidal constituents. These constituents were recognized in tilt data by using the Independent Component Analysis, and they are superimposed to the normal deformation trend of the area [65,66]. We estimated the azimuth of the tilt vector corresponding to the filtered signals of each tiltmeter, over sliding time windows with length equal to the period of each tidal constituent (Figure 7).

For both the Mm and Mf constituents, the azimuth directions, and hence the orientation of the ground oscillation planes, were nearly E–W, NE–SW and ESE–WNW for CMP, ECO and HDM site, respectively. These results confirm those obtained in [66] for the 2015–2016 time span, suggesting that, on average, the dominant oscillation pattern of the Campi Flegrei caldera has not changed in the last two years. However, at shorter time scales (less than 1 year), [66] pointed out that medium/long period filtered time series at the ECO tiltmeter shows a difference of about 60° in the azimuth values between data recorded in spring/summer and autumn/winter seasons. Moreover, the authors also noticed that the amplitude of the Mf constituent has itself a seasonal trend, being less or more evident according to the time of the year.

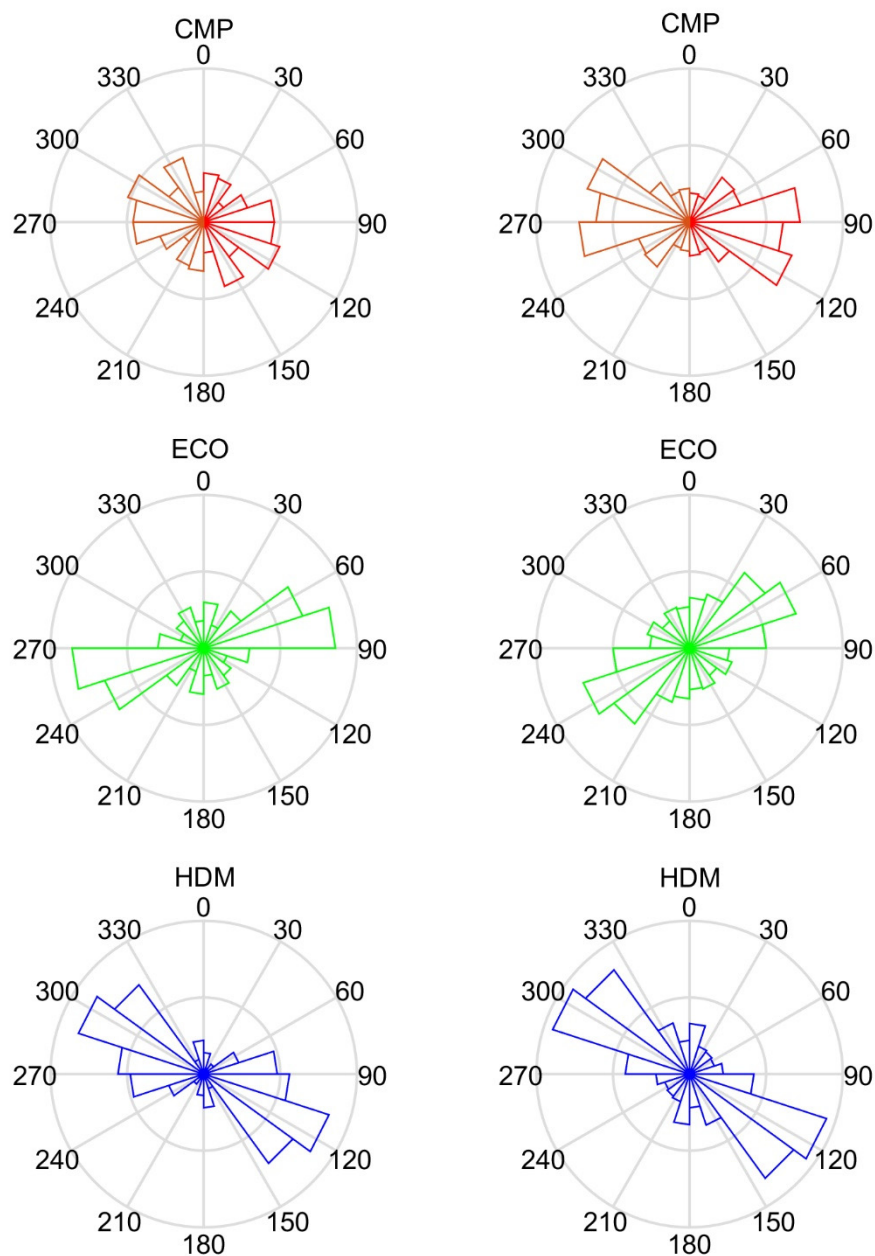


Figure 7. On the **left**, rose diagrams of the azimuths of the tilt signals corresponding to the Mm constituent (red = CMP, green = ECO, blue = HDM); on the **right** the same for the Mf constituent.

These observations, which surely deserve further investigation, lead us to deeply inspect the Mf time behavior of ECO data. Indeed, looking carefully at the filtered time series in the Mf band, four oscillating “packets” with large amplitude (and duration of about 45 days) clearly emerge over the background signal (Figure 8b): the first one has its maximum amplitude peak in October 2015 and it is detected only in the EW component, while the remaining three (with maximum amplitude peaks in April 2016, May 2017 and August 2018) occur on both the components, but with the largest amplitude on the EW. Hereafter, we will refer to these packets as LAO (Large Amplitude Oscillations). In Figure 8c we report the zoom of the temporal pattern of the tilt azimuth for a time window containing each of the four LAOs. We note that the azimuth has a slight variation of about 20° for the October 2015 LAO, while the other three LAOs exhibit azimuth rotations of about 90° .

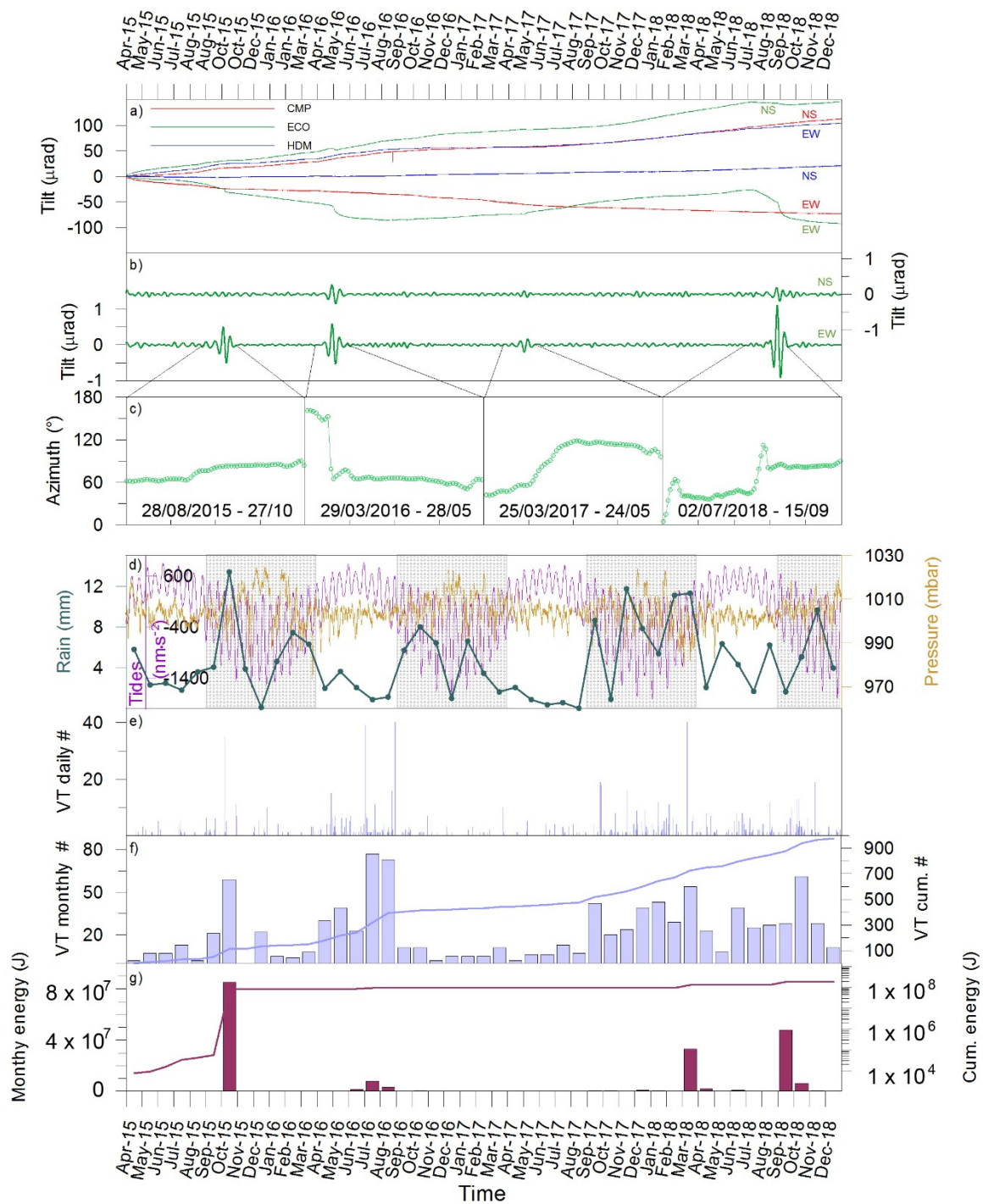


Figure 8. (a) Tilt time series from 1 April 2015 to 31 December 2018 for CMO, ECO and HDM (NS and EW components). The four vertical grey lines mark the maximum amplitude peak of the LAOs; (b) ECO tilt time series (NS and EW components) filtered in the period band corresponding to the Mf constituent; (c) temporal pattern of the azimuth of the LAOs over a two-month-long time window (start and end time indicated in the label); (d) solid Earth tides, atmospheric pressure and rainfall time series. The light-grey boxes in the background mark the wet season of the hydrological year [43]; (e) daily number of VTs; (f) monthly (bar plot) and cumulative (continuous line) number of VTs; (g) monthly (bar plot) and cumulative (continuous line) energy release of VTs.

To investigate possible relationships between tilt variations and seismic activity, we analysed the VT seismicity in the 2015–2018 time range. We calculated the daily, monthly and cumulative VT

number (Figure 8e,f) using the seismic catalogue compiled for a station, STH, located in the Solfatara area (<http://www.ov.ingv.it/ov/it/banche-dati.html>). In addition, the monthly and cumulative energy (Figure 8g) was obtained by applying the Gutenberg-Richter relationship for Campi Flegrei [35]:

$$\text{Log}E = 9.9 + 1.9 \cdot M_d \quad (1)$$

where E is the energy and M_d is the duration magnitude. From this analysis it emerges that a moderate seismic activity occurred up to August 2016. This phase was then followed by about one year of scarce seismicity. Since September 2017, moderate/high seismic rates are observed again. The strongest energy releases occurred in October 2015, July 2016, March 2018 and September 2018.

In Figure 8d, we provide the time series of the theoretical Earth tides generated by the code ATLANTIDA [67], atmospheric pressure (data from a barometric station located in Solfatara) and rainfall amount (data for Pozzuoli town, available at the URL <https://www.3bmeteo.com/meteo/pozzuoli/storico>).

Indeed, as recently shown in [43], the dynamics of Campi Flegrei are strictly related to both endogenous and exogenous phenomena. For example, the VT seismicity is driven by both variations in the deep magmatic feeding system as well as by tidal and hydrological cycles. Therefore, considering the joint influence of as many parameters as possible will help build a more complete scenario for the interpretation of the caldera dynamics. In this framework, our multiparametric observations evidence that:

(1) The October 2015 LAO occurs in the wet season of the hydrological year, when the Earth tide potential is approaching its seasonal minimum and the barometric pressure has major fluctuations. The LAO is concurrent with the most energetic VT swarm (7 October 2015), in a phase of high seismic energy release; its azimuth rotates about 20° . The LAO corresponds to the tilt anomaly (Figure 9) observed in the unfiltered time series during Time Interval I.

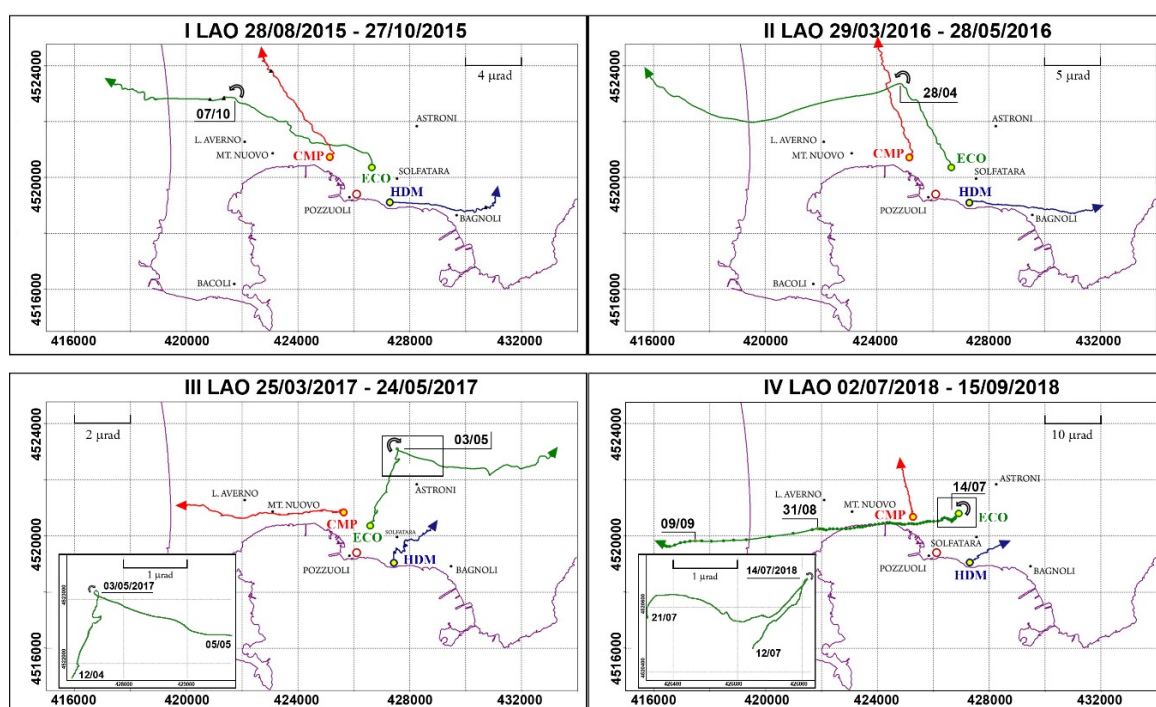


Figure 9. LAOs observed at ECO station in four different time spans discussed in the text. The tilt variations of 7 October 2015, 28 April 2016 (TR1), 3 May 2017 (TR2) and 14 July 2018 (TR3) are evidenced by a semicircular arrow pointing towards the reversal in tilting direction. The points superimposed to the ECO hodograph of the IV LAO mark the observed daily tilt, so the point spacing is proportional to the tilt rate. It can be observed how the tilt rate increases from 31 August 2018, stretching the soil towards the W until 9 September 2018, when the rate starts to decrease. The inset shows the zoom of the tilt reversals.

(2) The other three LAOs (April 2016, May 2017 and August 2018) occur in the dry season of the hydrological year, when Earth tide potential is approaching its seasonal maximum and the barometric pressure has minor fluctuations. They match three aseismic tilt reversal episodes (TR1, TR2 and TR3) detected in the unfiltered data (Figure 9) and occur in phases of low seismic energy release; their azimuths show a roughly 90° rotation.

In addition, although the present observations are limited only to three episodes, the amplitude of the LAOs corresponding to the aseismic tilt reversals seems to be related to the rain amount of the preceding wet season, as well as to the level of background seismicity. That is, tilt oscillations with larger amplitudes occur after wet seasons characterized by heavier rainfalls and higher VT rate. However, the time record of the present dataset is still too short to assess a cause-effect relationship and more data need to be gathered over a longer time interval to confirm any possible trends.

To summarize, the occurrence (and maybe the magnitude too) of the LAO episodes at ECO site appears to be driven by external factors such as rainfall amount and Earth tidal and barometric pressure cycles.

3.2. Ischia Island

The Ischia Monitoring Tiltmeter Network of INVG-OV has been operating on the island since the end of April 2015 and includes three tiltmeters (ISC, BRN, FOR) surrounding Mt Epomeo (Figure 10a). The sensors (model Lily Self-Leveling Borehole) are placed at the bottom of the well, at depths of about 25 m, to record tilt signals not affected by surface thermal disturbances. Ground tilt variations are measured along two orthogonal directions NS and EW; they are recorded with a sampling rate of 1 sample (defined as the average of 8000 readings) per minute.

The INGV-OV seismic network of Ischia Island originally composed of only permanent stations (Figure 1), was massively upgraded after the Md 4.0 EQ2017 by adding several mobile installations [10]. The analog and digital permanent dataloggers are equipped with short-period 1 Hz (Mark L4C) and three-component broadband seismometers (Guralp CMG40T), respectively. The mobile stations are assembled with three-component short-period (Lennartz LE-3Dlite) and broadband (Lennartz LE3D/5s) sensors. The seismic network is still under development, so for the most updated configuration refer to the URL www.ov.ingv.it [10].

Ground tilt pattern recorded in the time span 1 June 2015–21 August 2017 shows a well-defined polarization toward the NNW, but with a greater inclination in the northeastern sector (Figure 10a). The EQ2017 (20:57:52, UTC+2) interrupted this trend because, after it, the polarization of the tilting directions turned clockwise towards the NNE (Figure 10a). The earthquake was also well detected by the tiltmeter monitoring network and was accompanied by the rotation of the tilting directions. In the following, we summarize the results of the analysis of the 10-minute long time series recorded before and after the seismic event. At ISC station, located about 3 km ESE from the epicentral area (Figure 10a), the first tilt rotation occurred in the SSW direction one minute before the event (20:57). A second change in the SW direction took place during the event itself (20:58) and finally the site tilted permanently to NW (20:59 and 21:03) (Figure 10d).

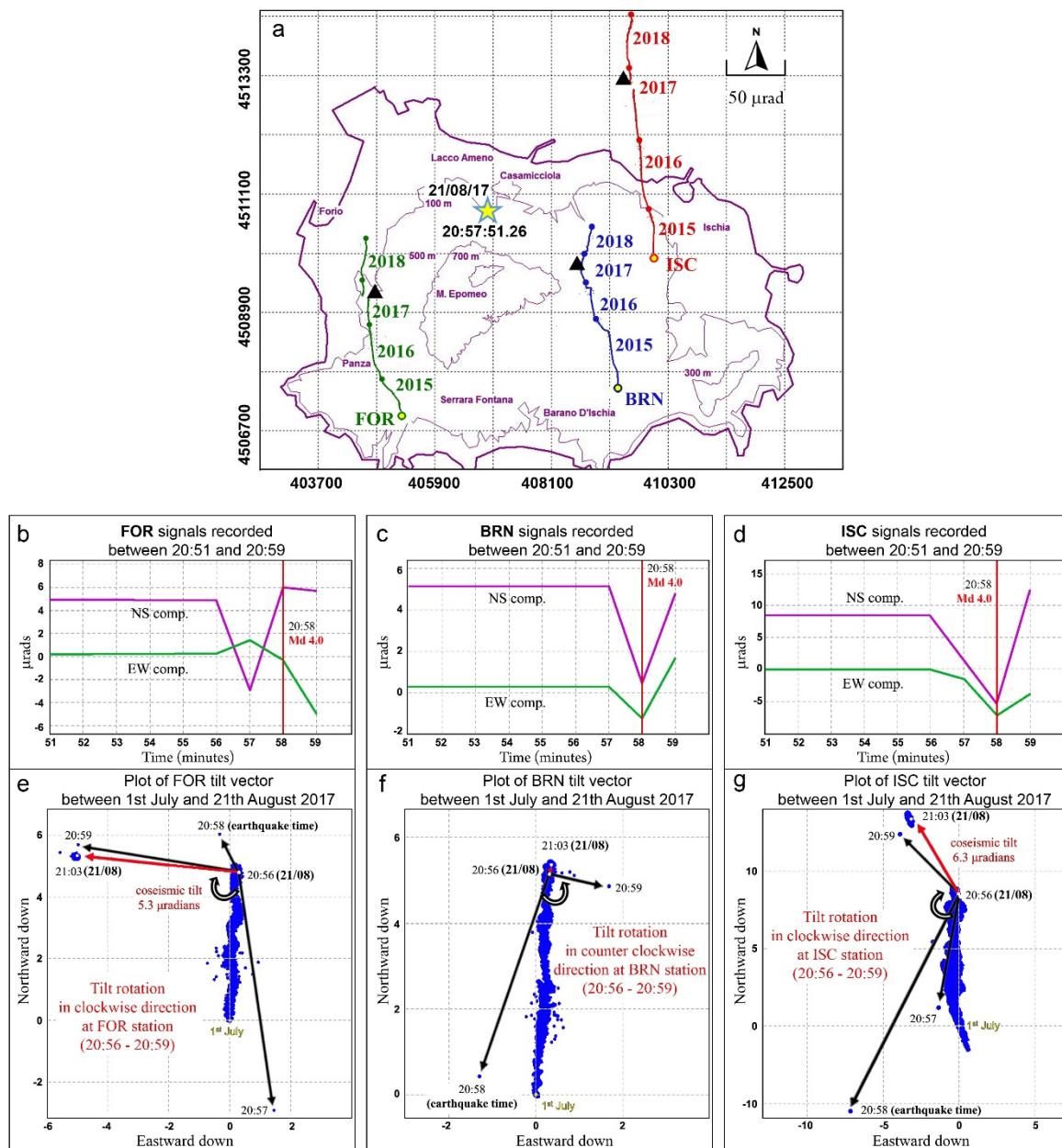


Figure 10. (a) Schematic map of Ischia Island, superimposed on a grid representing the two-dimensional plane of ground inclinations, in which each mesh is equivalent to a tilt variation of $50 \mu\text{rad}$. The three sites ISC, FOR and BRN are distinguished by different colors (red, green and blue, respectively). The hodographs observed at each site in the time span 1 June 2015–31 December 2018 show a well-defined polarization towards the NNW but with a greater inclination in the northeastern sector. (The epicenter of the EQ2017 is marked with a yellow star). (b–d) NS and EW components of the tilt signals observed at FOR, BRN and ISC in the time interval 20:51–20:59 (red vertical lines mark the EQ2017). (e–g) Plots of the tilt vectors recorded at FOR, BRN and ISC between 1 July 2017 and 21 August 2017. The red arrows indicate the permanent coseismic offset and the black arrows indicate the tilt direction observed during the EQ2017.

During the seismic event, a clear clockwise rotation of the tilting direction was observed (Figure 10g). The two clouds (blue color, Figure 10g) of points visible in the hodograph represent the tilt variation recorded from 1 July 2017 to 21 August 2017. The spatial concentrations of points are separated at the onset of the earthquake and this spatial offset is owed to a permanent coseismic deformation of $6.3 \mu\text{rad}$ towards the NW. At FOR station, located about 4 km SW of the epicenter (Figure 10a),

the first tilt rotation occurred one minute before the event (20:57) but in the SSE direction. A second change in the NNW direction then occurred simultaneously with the event (20:58), and subsequently it tilted permanently to the W-NNW (20:59 and 21:03) (Figure 10b). This time a marked clockwise rotation of the tilting direction was observed (Figure 10e). The tiltmeter recorded a coseismic tilt of 5.3 μ rad towards the W. Finally, at BRN station, located about 3 km SE of the epicenter (Figure 10a), the rotation occurred in the SSW direction only during the event itself (20:58) and then to the ESE (20:59), just after the ground inclination reentered the cloud of points aligned to the NNE tilting direction (21:03) (Figure 10c). Similar to station FOR, a clear counterclockwise rotation of the tilting direction was observed (Figure 10f). The BRN tiltmeter did not record any co-seismic tilt.

Considering the structural lineaments of the island, the coseismic tilt of ISC is likely related to the subsidence of Mt Epomeo and therefore to the deformation of the epicentral area itself. The one recorded by the station FOR, located in the SW sector, is attributable to the position of the sensor itself, as it is located at the base of a system of faults that dips to the W and which are well lubricated by subsurface water circulation. The hinge of the deformation recorded in the time interval 20:51–20:59 seems to be at BRN, as it is the only one of the three tiltmeters to undergo a rotation that does not end with a coseismic tilt (Figure 10f). Since this jump is permanent, i.e. it remains after the earthquake, it can be assumed that the sensor was rotated counterclockwise by about a tenth of a degree at the same time as the seismic wave is passed through.

The analysis of tilt data at short time scales was complemented by the study of medium/long term ground oscillation patterns. We narrow-band filtered the entire tilt time series around the periods of the Mm and Mf tidal constituents, by using the same techniques applied to the Campi Flegrei data. Considering the average direction over the investigated time interval (June 2015–December 2018), the orientations of the ground oscillation planes corresponding to the Mm period are nearly NNW-SSE for the ISC and BRN sites, and WNW-ESE for FOR. In the Mf band, the tilt azimuth is oriented NNW-SSE for all the three sites (Figure 11). Some LAO episodes appear on the filtered time series, the most significant is associated with the EQ2017 and detected at ISC and FOR sites (Figure 12c–e).

Possible correlations with the seismicity occurring in the time span 2015–2018 were investigated by calculating the monthly and cumulative earthquake number and energy (Figure 12d,e) using the seismic catalogue of OC9 station, located in the area of Casamicciola (<http://www.ov.ingv.it/ov/it/banche-dati.html>). As one can note from Figure 12d, the seismicity rate is very low. The most intense activity occurred in August 2017 (28 earthquakes) when the Md 4.0 EQ2017 struck the island. This sequence gave rise to the highest release in seismic energy (Figure 12e). Since that date, only a few low-energy earthquakes has been detected.

From a first joint analysis of the tilt and seismic data, only the EQ2017 is concomitant with a tilt rotation, while the other small VT sequences do not correspond to any anomalies in the tilt signals. Instead, from the kinematics inferred by the tilt patterns recorded on Ischia during the strong EQ2017, emerges a very complex picture of the dynamics. At BRN station, moreover, a magnetic anomaly contemporary to the earthquake occurred, with the recorded magnetic declination signal jumping 0.11°, equivalent to the annual variation of this component of the Earth's magnetic field. This issue be further studied by using conceptual models that can link the rare seismic activity with conspicuous effects of ground deformation detected by tiltmeters.

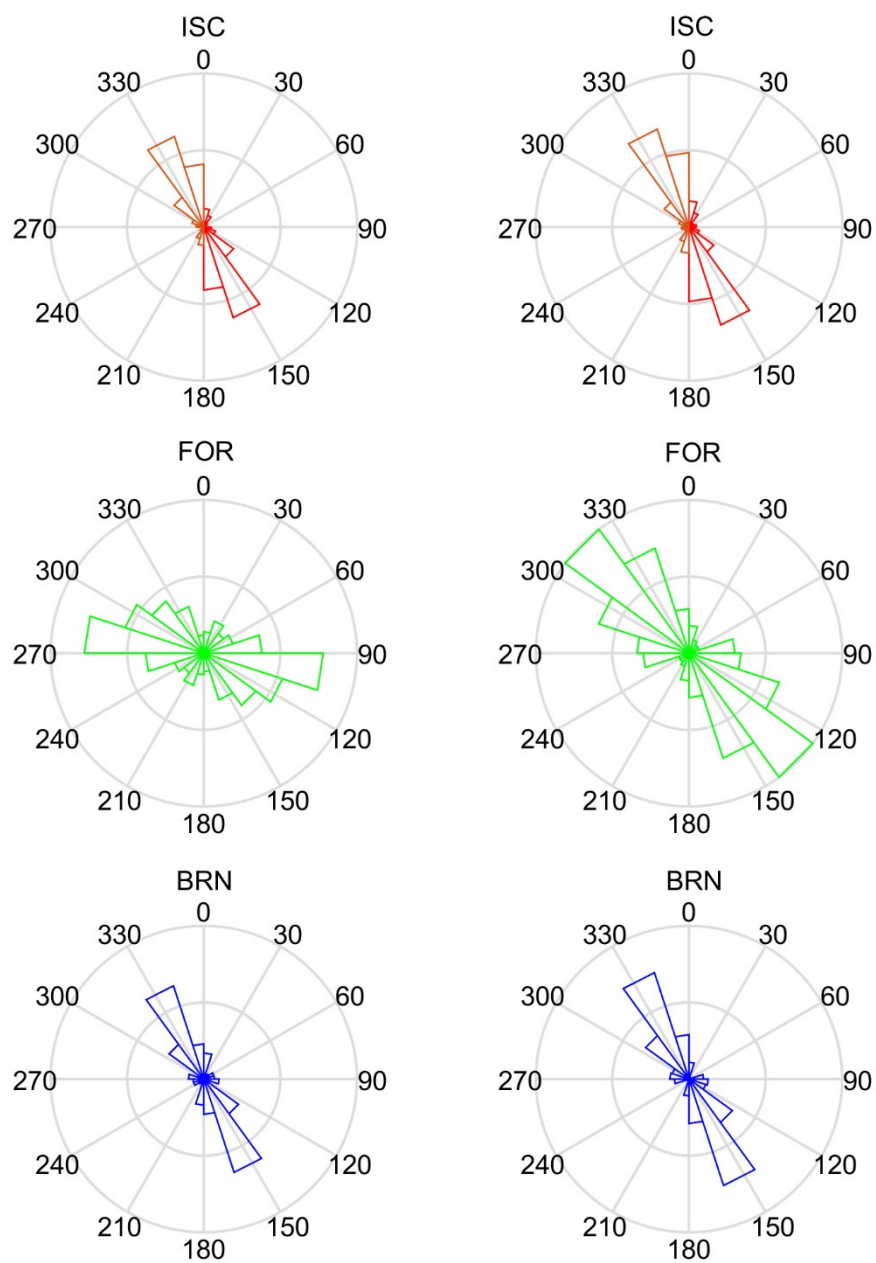


Figure 11. On the **left**, rose diagrams of the azimuths of the tilt signals corresponding to the Mm constituent (red = ISC, green = FOR, blue = BRN); on the **right** the same for the Mf constituent.

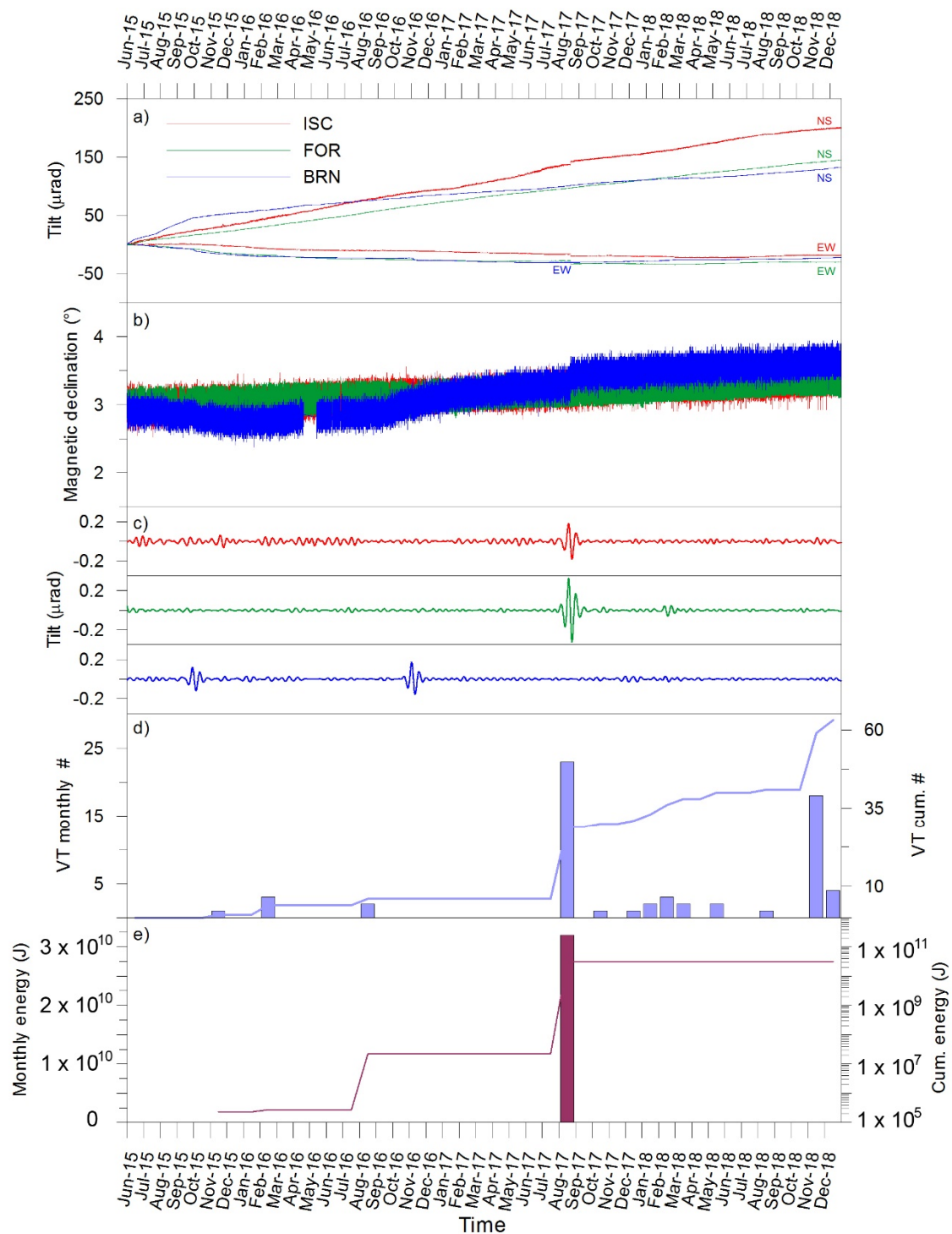


Figure 12. (a) Tilt time series from 1 June 2015 to 31 December 2018 for ISC, FOR and BRN (NS and EW components); (b) magnetic declination recorded at the three instruments; (c) tilt time series ISC, FOR and BRN (EW components) filtered in the period band corresponding to the Mf constituent; (d) monthly (bar plot) and cumulative (continuous line) number of VTs; (e) monthly (bar plot) and cumulative (continuous line) energy release of VTs.

4. Discussion and Conclusions

The data analysis over the last 15 years at Campi Flegrei and Ischia has revealed interesting links between tilt and seismic signals that suggest a common source underlying the phenomenology.

The role played by Earth tides in modulating the ground deformation arises from the analysis of the tilt data in the medium/long (fortnightly and monthly) period band, over the entire nearly 4-year interval 2015–2018. In fact, both at Campi Flegrei and Ischia island, the results show that the ground response occurs in an oscillatory deformation pattern with the same periodicity of the corresponding tidal constituent. However, at Ischia the direction of the tidal oscillation planes (nearly SSE-NNW at all the sites) remains almost constant over the time and is roughly aligned with the main direction of the local deformation field, thus indicating a predominant effect of the local kinematics. On the contrary, at Campi Flegrei, depending on the site, the tilt azimuth in the tidal band may undergo cyclic rotations caused by external triggering and it superimposed on the ground deformation trend related to the endogenous dynamics.

At Ischia Island, the preliminary observations of the contemporary occurrence of tilt anomalies, high-energy earthquakes, LAOs and variations of the magnetic declinations require undertaking an accurate and detailed study of the tidal, barometric and hydrological cycles, as has been done for Campi Flegrei [43,66]. Indeed, additional elements are necessary in order to establish a link between different phenomenologies and to identify a common source, whether exogenous or endogenous.

At Campi Flegrei, the most intriguing observation is that the tilt variations repeatedly occurred over the investigated time interval, sometimes accompanied by earthquakes (October 2006, March 2010, October 2015), and sometimes aseismically. Since 2015, with the availability of the borehole instruments, we highlighted that these episodes, at least for the ECO site, correspond to the large oscillations (LAO) in the tilt signals on the fortnightly time scale. A clue for the interpretation of this phenomenon is to be searched in the fluctuations of the fluid-pore pressure of the medium. These changes can induce rotation of the tilt directions, as has similarly been found elsewhere [68–71]. On macroscopic spatial scale, the fluid-pore pressure is strictly controlled by the local stress and fluid flow regime [72]. Exogenous factors such as Earth tide cycles, barometric pressure variations and rainfall can modify either the stress field or the ground water content, thus in turn causing, at microscopic spatial scale, the opening/closing of voids in the rocks, and changes in permeability and pore pressure [43,73–75]. On the other hand, a variation of the fluid-pore pressure can be induced by endogenous factors, e.g. fluid injections from a hydrothermal/magmatic reservoir [76,77]. The observed modality of occurrence of the LAO episodes lead us to hypothesize that they are induced by non-volcanic external sources (rather than endogenous ones) which periodically modulate the stress field and the water content in the shallow crust. This interpretation is in line with [66] who found that at Campi Flegrei the tidal tilting is controlled by the local stress field distribution and by the rheology. Thus, the LAOs reflect the ground response to a mixing of exogenous sources; depending on the boundary conditions (minima/maxima of the tidal potential, seasonality of the hydrological years and barometric pressure cycles) they are associated either with tilt anomalies accompanied by intense seismic activity or with aseismic tilt reversals. From this point of view the tilt variations observed in the unfiltered time series can be considered as the fingerprints of the rotation of the oscillation planes that occurs on tidal time scales.

The lack of clear LAO episodes at CMP and HDM tiltmeters suggests that these two sites are less sensitive to stress and fluid regime variations. A possible site effect would be a reasonable explanation, since [66] have already pointed out the difference in responses of the three sites. Indeed ECO is installed close to a local system of fractures (see [78]), as well as in the neighborhood of the hydrothermal system of Solfatara. This latter condition plays a particularly important role because the presence of fluid can enhance the effects induced by the lunar tidal constituents, such as the modulation of the geophysical signals on the typical tidal time scales [75,79].

On hourly time scales, the other interesting aspect arising from our study regards the tilt anomalies concurrent with the most energetic earthquakes. Although it is extremely difficult to quantify a cause-effect relationship, this peculiar behavior deserves further investigation in order to establish its systematic nature. More observations are required in order to gather a data set numerically significant from a statistical point of view. However, it is noteworthy that at Campi Flegrei, the duration of the tilt offsets immediately preceding the major VTs of the October 2015 sequence are comparable with

the average inter-arrival times (less than 15 min) statistically estimated for the VT swarms [43,80]. Such behavior could be indicative of the existence of characteristic time and spatial length scales related to the VT generation mechanism and source dimension. This would not be surprising, since similar characteristic length scales have been found for the LP events that occurred in 2006 [40].

In conclusion, the careful investigation of the possible links between ground tilt and seismic activity, as well as with exogenous factors, is extremely useful to define the background state of the volcanoes and to correctly interpret the observed anomalies in tilt and seismic data. This is particularly relevant for improving both knowledge of the volcanic processes and monitoring. A departure from the background state would be an important indicator of the possible variations of internal dynamics, to be taken into account for volcanic surveillance.

Author Contributions: Conceptualization, S.P., C.R. and M.F.; Methodology, C.R., I.A., S.P., M.F. and C.D.G.; Validation, C.R., I.A., M.F. and S.P.; Resources, S.P., C.R. and M.F.; Writing—Original Draft Preparation, C.R., I.A., M.F. and S.P.; Writing—Review & Editing, I.A., S.P., C.R. and M.F.; Visualization I.A.; Supervision, I.A., C.R., S.P. and M.F.

Funding: This research received no external funding.

Acknowledgments: The authors would like to thank Vincenzo Augusti for his efforts to providing regular maintenance and calibration of the tiltmeter network.

Conflicts of Interest: The authors declare no conflict of interest.

References

1. Genco, R.; Ripepe, M. Inflation-deflation cycles revealed by tilt and seismic records at Stromboli volcano. *Geophys. Res. Lett.* **2010**, *37*, 12. [CrossRef]
2. Voight, B.; Hoblitt, R.P.; Clarke, A.B.; Lockhart, A.B.; Miller, A.D.; Lynch, L.; McMahon, J. Remarkable cyclic ground deformation monitored in real-time on Montserrat, and its use in eruption forecasting. *Geophys. Res. Lett.* **1998**, *25*, 3405–3408. [CrossRef]
3. Gambino, S. Tilt offset associated with local seismicity: The Mt. Etna January 9, 2001 seismic swarm. *Open Geosci.* **2016**, *8*, 514–522. [CrossRef]
4. Anderson, K.; Lisowski, M.; Segall, P. Cyclic ground tilt associated with the 2004–2008 eruption of Mount St. Helens. *J. Geophys. Res.* **2010**, *115*, B11201. [CrossRef]
5. Ricco, C.; Aquino, I.; Borgstrom, S.E.; Del Gaudio, C. 19 years of tilt data on Mt. Vesuvius: State of the art and future perspectives. *Ann. Geophys.* **2013**, *56*, S0453.
6. Ricco, C.; Aquino, I.; Del Gaudio, C. Ground tilt monitoring at Phlegraean Fields (Italy): A methodological approach. *Ann. Geophys.* **2003**, *46*, 1297–1314.
7. Ricco, C.; Aquino, I.; Borgstrom, S.E.; Del Gaudio, C. A study of tilt change recorded from July to October 2006 at the Phlegraean Fields (Naples, Italy). *Ann. Geophys.* **2007**, *50*, 661–674.
8. Ricco, C.; Aquino, I.; Augusti, V.; D’Auria, L.; Del Gaudio, C.; Scarpato, G. Improvement and development of the tiltmetric monitoring networks of Neapolitan volcanoes. *Ann. Geophys.* **2018**, *61*, SE114. [CrossRef]
9. La Rocca, M.; Galluzzo, D. Seismic monitoring of Campi Flegrei and Mt. Vesuvius by stand alone instruments. *Ann. Geophys.* **2015**, *58*, S0544.
10. D’Auria, L.; Giudicepietro, F.; Tramelli, A.; Ricciolino, P.; Lo Bascio, D.; Orazi, M.; Martini, M.; Peluso, R.; Scarpato, G.; Esposito, A. The seismicity of Ischia Island. *Seismol. Res. Lett.* **2018**, *89*, 1750–1760. [CrossRef]
11. Bianco, F.; Cusano, P.; Petrosino, S.; Castellano, M.; Buonocunto, C.; Capello, M.; Del Pezzo, E. Small-aperture array for seismic monitoring of Mt. Vesuvius. *Seismol. Res. Lett.* **2005**, *76*, 344–355. [CrossRef]
12. Del Pezzo, E.; Bianco, F.; Castellano, M.; Cusano, P.; Galluzzo, D.; La Rocca, M.; Petrosino, S. Detection of seismic signals from background noise in the area of Campi Flegrei: Limits of the present seismic monitoring. *Seismol. Res. Lett.* **2013**, *84*, 190–198. [CrossRef]
13. De Lauro, E.; De Martino, S.; Falanga, M.; Petrosino, S. Fast wavefield decomposition of volcano-tectonic earthquakes into polarized P and S waves by independent component analysis. *Tectonophysics* **2016**, *690*, 355–361. [CrossRef]

14. Capuano, P.; De Lauro, E.; De Martino, S.; Falanga, M.; Petrosino, S. Convolutional independent component analysis for processing massive datasets: A case study at Campi Flegrei (Italy). *Nat. Hazards* **2017**, *86*, 417–429. [\[CrossRef\]](#)
15. Di Vito, M.A.; Isaia, R.; Orsi, G.; Southon, J.; D'Antonio, M.; de Vita, S.; Pappalardo, L.; Piochi, M. Volcanism and deformation since 12,000 years at the Campi Flegrei caldera (Italy). *J. Volcanol. Geotherm. Res.* **1999**, *91*, 221–246. [\[CrossRef\]](#)
16. Orsi, G.; Civetta, L.; D'Antonio, M.; Di Girolamo, P.; Piochi, M. Step-filling and development of a three-layer magma chamber: The Neapolitan yellow tuff case history. *J. Volcanol. Geotherm. Res.* **1995**, *67*, 291–312. [\[CrossRef\]](#)
17. Orsi, G.; de Vita, S.; Di Vito, M. The restless, resurgent Campi Flegrei nested caldera (Italy): Constraints on its evolution and configuration. *J. Volcanol. Geotherm. Res.* **1996**, *74*, 179–214. [\[CrossRef\]](#)
18. Pappalardo, L.; Civetta, L.; D'Antonio, M.; Deino, A.L.; Di Vito, M.A.; Orsi, G.; Carandente, A.; de Vita, S.; Isaia, R.; Piochi, M. Chemical and isotopic evolution of the Phlegraean magmatic system before the Campanian Ignimbrite (37 ka) and the Neapolitan yellow tuff (12 ka) eruptions. *J. Volcanol. Geotherm. Res.* **1999**, *91*, 141–166. [\[CrossRef\]](#)
19. Piochi, M.; Civetta, L.; Orsi, G. Mingling in the magmatic system of Ischia (Italy) in the past 5 Ka. *Mineral. Petrol.* **1999**, *66*, 227–258. [\[CrossRef\]](#)
20. Acocella, V.; Funicello, R. The interaction between regional and local tectonics during resurgent doming: The case of the island of Ischia, Italy. *J. Volcanol. Geotherm. Res.* **1999**, *88*, 109–123. [\[CrossRef\]](#)
21. Piochi, M.; Mastrolorenzo, G.; Pappalardo, L. Magma ascent and eruptive processes from textural and compositional features of Monte Nuovo pyroclastic products, Campi Flegrei, Italy. *Bull. Volcanol.* **2005**, *67*, 663–678. [\[CrossRef\]](#)
22. Sacchi, M.; Alessio, G.; Aquino, I.; Esposito, E.; Molisso, F.; Nappi, R.; Porfido, S.; Violante, C. Risultati preliminari della campagna oceanografica CAFE_07—Leg 3 nei Golfi di Napoli e Pozzuoli, Mar Tirreno Orientale. *Quad. Geofis.* **2009**, *64*, 1–30.
23. De Vita, S.; Sansivero, F.; Orsi, G.; Marotta, E.; Piochi, M. Volcanological and structural evolution of the Ischia resurgent caldera (Italy) over the past 10 k.y. In *Stratigraphy and Geology of Volcanic Areas*; Groppelli, G., Viereck-Goette, L., Eds.; GeoScienceWorld: McLean, VA, USA, 2010; Volume 464, pp. 193–239.
24. Sacchi, M.; Pepe, F.; Corradino, M.; Insinga, D.D.; Molisso, F.; Lubritto, C. The Neapolitan yellow tuff caldera offshore the Campi Flegrei: Stratal architecture and kinematic reconstruction during the last 15 ky. *Mar. Geol.* **2014**, *354*, 15–33. [\[CrossRef\]](#)
25. Civetta, L.; Orsi, G.; Pappalardo, L.; Fischer, R.V.; Heiken, G. Geochemical zoning, mingling, eruptive dynamics and the positional processes: The Campanian Ignimbrite, Campi Flegrei caldera, Italy. *J. Volcanol. Geotherm. Res.* **1997**, *75*, 183–219. [\[CrossRef\]](#)
26. Deino, A.L.; Orsi, G.; de Vita, S.; Piochi, M. The age of the Neapolitan yellow tuff caldera-forming eruption (Campi Flegrei caldera—Italy) assessed by $^{40}\text{Ar}/^{39}\text{Ar}$ dating method. *J. Volcanol. Geotherm. Res.* **2004**, *133*, 157–170. [\[CrossRef\]](#)
27. D'Oriano, C.; Poggianti, E.; Bertagnini, A.; Cioni, R.; Landi, P.; Polacci, M.; Rosi, M. Changes in eruptive style during the A.D. 1538 Monte Nuovo eruption (Phlegrean Fields, Italy): The role of syn-eruptive crystallization. *Bull. Volcanol.* **2005**, *67*, 601–621. [\[CrossRef\]](#)
28. Di Vito, M.A.; Acocella, V.; Aiello, G.; Barra, D.; Battaglia, M.; Carandente, A.; Del Gaudio, C.; de Vita, S.; Ricciardi, G.P.; Ricco, C.; Scandone, R.; Terrasi, F. Magma transfer at Campi Flegrei caldera (Italy) before the 1538 AD eruption. *Sci. Rep.* **2016**, *6*, 32245. [\[CrossRef\]](#)
29. Morhange, C.; Marriner, N.; Laborel, J.; Todesco, M.; Oberlin, C. Rapid sea-level movements and noneruptive crustal deformations in the Phlegrean Fields caldera, Italy. *Geology* **2006**, *34*, 93–96. [\[CrossRef\]](#)
30. Isaia, R.; Marianelli, P.; Sbrana, A. Caldera unrest prior to intense volcanism in Campi Flegrei (Italy) at 4.0 ka B.P.: Implications for caldera dynamics and future eruptive scenarios. *Geophys. Res. Lett.* **2009**, *36*. [\[CrossRef\]](#)
31. Del Gaudio, C.; Aquino, I.; Ricciardi, G.P.; Ricco, C.; Scandone, R. Unrest episodes at Phlegrean Fields: A reconstruction of vertical ground movements during 1905–2009. *J. Volcanol. Geotherm. Res.* **2010**, *195*, 48–56. [\[CrossRef\]](#)
32. Bellucci, F.; Woo, J.; Kilburn, C.; Rolandi, G. Ground deformation at Campi Flegrei, Italy: Implications for hazard assessment. *Geolog. Soc. Lond. Spec. Publ.* **2006**, *269*, 141–157. [\[CrossRef\]](#)

33. Civetta, L.; Del Gaudio, C.; De Vita, S.; Di Vito, M.A.; Orsi, G.; Petrazzuoli, S.; Ricciardi, G.; Ricco, C. Volcanism and resurgence in the densely populated campi Flegrei nested caldera. *Period. Mineral.* **1995**, *44*, 135–136.
34. Del Gaudio, C.; Ricciardi, G.; Ricco, C.; Sepe, V.; Berrino, G.; Riccardi, U.; d’Errico, V.; La Rocca, A. Phlegrean Fields. Ground deformations. In *Data Related to Eruptive Activity, Unrest Phenomena and Other Observations on the Italian Active Volcanoes. Geophysical Monitoring of the Italian Active Volcanoes 1993–1995*; Gasparini, P., Ed.; Acta Vulcanologica: Pisa, Italy, 1998; Volume 10, pp. 103–107.
35. Orsi, G.; Civetta, L.; Del Gaudio, C.; de Vita, S.; Di Vito, M.A.; Isaia, R.; Petrazzuoli, S.M.; Ricciardi, G.P.; Ricco, C. Short-term ground deformations and seismicity in the resurgent Campi Flegrei caldera (Italy): An example of active block-resurgence in a densely populated area. *J. Volcanol. Geotherm. Res.* **1999**, *91*, 415–451. [[CrossRef](#)]
36. Del Gaudio, C.; Aquino, I.; Ricco, C.; Serio, C. Monitoraggio geodetico dell’area vulcanica napoletana: Risultati della Livellazione Geometrica di Precisione eseguita ai Campi Flegrei a settembre 2008. *Quad. Geofis.* **2009**, *2009*, 66.
37. Saccorotti, G.; Petrosino, S.; Bianco, F.; Castellano, M.; Galluzzo, D.; La Rocca, M.; Del Pezzo, E.; Zaccarelli, L.; Cusano, P. Seismicity associated with the 2004–2006 renewed ground uplift at campi flegrei caldera, Italy. *Phys. Earth Planet. Inter.* **2007**, *165*, 14–24. [[CrossRef](#)]
38. Cusano, P.; Petrosino, S.; Saccorotti, G. Hydrothermal origin for sustained long-period (LP) activity at Campi Flegrei Volcanic Complex, Italy. *J. Volcanol. Geotherm. Res.* **2008**, *177*, 1035–1044. [[CrossRef](#)]
39. Falanga, M.; Petrosino, S. Inferences on the source of long-period seismicity at Campi Flegrei from polarization analysis and reconstruction of the asymptotic dynamics. *Bull. Volcanol.* **2012**, *74*, 1537–1551. [[CrossRef](#)]
40. De Lauro, E.; Falanga, M.; Petrosino, S. Study on the long-period source mechanism at Campi Flegrei (Italy) by a multi-parametric analysis. *Phys. Earth Planet. Inter.* **2012**, *206*, 16–30. [[CrossRef](#)]
41. Capuano, P.; De Lauro, E.; De Martino, S.; Falanga, M. Detailed investigation of long-period activity at Campi Flegrei by convolutive independent component analysis. *Phys. Earth Planet. Inter.* **2016**, *253*, 48–57. [[CrossRef](#)]
42. D’Auria, L.; Giudicepietro, F.; Aquino, I.; Borriello, G.; Del Gaudio, C.; Lo Bascio, D.; Martini, M.; Ricciardi, G.P.; Ricciolino, P.; Ricco, C. Repeated fluid-transfer episodes as a mechanism for the recent dynamics of Campi Flegrei caldera (1989–2010). *J. Geophys. Res.* **2011**, *116*, B04313. [[CrossRef](#)]
43. Petrosino, S.; Cusano, P.; Madonna, P. Tidal and hydrological periodicities of seismicity reveal new risk scenarios at Campi Flegrei caldera. *Sci. Rep.* **2018**, *8*, 13808. [[CrossRef](#)] [[PubMed](#)]
44. Di Luccio, F.; Pino, N.A.; Piscini, A.; Ventura, G. Significance of the 1982–2014 Campi Flegrei seismicity: Preexisting structures, hydrothermal processes, and hazard assessment. *Geophys. Res. Lett.* **2015**, *42*, 7498–7506. [[CrossRef](#)]
45. Vezzoli, L. *Island of Ischia*; Quad. de La ricerca scientifica; CNR, Progetto Finalizzato Geodinamica 10: Roma, Italy, 1988; Volume 114, p. 133.
46. Bruno, P.P.; De Alteriis, G.; Florio, G. The western undersea section of the Ischia volcanic complex (Italy, Tyrrhenian sea) inferred by marine geophysical data. *Geophys. Res. Lett.* **2002**, *29*, 57. [[CrossRef](#)]
47. Tibaldi, A.; Vezzoli, L. Late Quaternary monoclinial folding induced by caldera resurgence at Ischia, Italy. In *Forced Folds and Fractures*; Cosgrove, J.W., Ameen, M.S., Eds.; Geological Society, London, Special Publications: London, UK, 2000; Volume 169, pp. 103–113.
48. Tibaldi, A.; Vezzoli, L. A new type of volcano flank failure: The resurgent caldera sector collapse, Ischia, Italy. *Geophys. Res. Lett.* **2004**, *31*, L14605. [[CrossRef](#)]
49. Acocella, V.; Funicello, R. Transverse structures and volcanic activity along the Tyrrhenian margin of central Italy. *Boll. Soc. Geol. It.* **2002**, *1*, 739–747.
50. Nappi, R.; Alessio, G.; Bellucci Sessa, E. A case study comparing landscape metrics to geologic and seismic data from the Ischia Island (Southern Italy). *Appl. Geomat.* **2010**, *2*, 73–82. [[CrossRef](#)]
51. Chiesa, S.; Poli, S.; Vezzoli, L. Studio dell’ultima eruzione storica dell’isola di Ischia. *Boll. GNV* **1986**, *1*, 153–166.
52. Iacono, A. La Guerra d’Ischia. In *De Bello Neapolitano*; Pontano, G., Ed.; Quaderni dell’Accademia Pontaniana: Napoli, Italy, 1996; Volume 19, pp. 1–90.

53. Achilli, V.; Al-Bayari, O.; Artese, G.; Borgstrom, S.; Capone, M.; Del Gaudio, C.; Gandolfi, S.; Macchiavelli, N.; Ricciardi, G.; Ricco, C.; et al. GPS Measurements in the Neapolitan volcanic area. *Phys. Chem. Earth Part A* **2000**, *25*, 705–711. [\[CrossRef\]](#)
54. Gabriel, A.K.; Goldstein, R.M.; Zebker, H.A. Mapping small elevation changes over large areas: Differential radar interferometry. *J. Geophys. Res. Solid Earth* **1989**, *94*, 9183–9191. [\[CrossRef\]](#)
55. Manzo, M.; Ricciardi, G.P.; Casu, F.; Ventura, G.; Zeni, G.; Borgström, S.; Berardino, P.; Del Gaudio, C.; Lanari, R. Surface deformation analysis in the Ischia Island (Italy) based on spaceborne radar interferometry. *J. Volcanol. Geotherm. Res.* **2006**, *151*, 399–416. [\[CrossRef\]](#)
56. Sepe, V.; Atzori, S.; Ventura, G. Subsidence due to crack closure and depressurization of hydrothermal systems: A case study from Mt. Epomeo (Ischia Island, Italy). *Terra Nova* **2007**, *19*, 127–132. [\[CrossRef\]](#)
57. Cubellis, E.; Luongo, G. *Il Terremoto del 28 Luglio 1883 a Casamicciola Nell'isola d'Ischia. Parte III "Il Contesto Fisico"*; Monografia n.1, Servizio Sismico Nazionale, Istituto Poligrafico e Zecca dello Stato: Roma, Italy, 1998; pp. 49–123.
58. Luongo, G.; Carlino, S.; Cubellis, E.; Delizia, I.; Iannuzzi, R.; Obrizzo, F. *Il Terremoto di Casamicciola del 1883: Una Ricostruzione Mancata*; Alfa Tipografia: Napoli, Italy, 2006; p. 64.
59. Alessio, G.; Esposito, E.; Ferranti, L.; Mastrolorenzo, G.; Porfido, S. Correlazione tra sismicità ed elementi strutturali nell'isola di Ischia. *Il Quaternario. It. J. Quat. Sci.* **1996**, *9*, 303–308.
60. Esposito, E.; Porfido, S.; Vittori, E. Earthquake hazard in the Island of Ischia (Campania, Italy). *Geophys. Res. Abstr.* **2006**, *8*, 08573.
61. Applied Geomechanics Incorporated (AGI). *LILY Self-Leveling Borehole Tiltmeter. User's Manual no. B-05-1003*; AGI: Roma, Italy, 2005; Rev. D.
62. Jewell Instruments. *LILY Self-Leveling Borehole Tiltmeter. User's Manual no. B-05-1003*; Jewell Instruments: Manchester, NH, USA, 2013; Rev. G.
63. Aquino, I.; Ricco, C.; Del Gaudio, C.; Augusti, V.; Scarpato, G. Potenziamento delle reti tiltmetriche dell'area vulcanica campana: Rapporto sull'attività svolta nell'ambito del Progetto VULCAMED. *Rapporti Tec. INGV* **2016**, *348*, 51.
64. Zadro, M.; Braitenberg, C. Measurements and interpretations of tilt-strain gauges in seismically active areas. *Earth Sci. Rev.* **1999**, *47*, 151–187. [\[CrossRef\]](#)
65. Bottiglieri, M.; Falanga, M.; Tammara, U.; De Martino, P.; Obrizzo, F.; Godano, C.; Pingue, F. Characterization of GPS time series at the Neapolitan volcanic area by statistical analysis. *J. Geophys. Res.* **2010**, *115*, B10416. [\[CrossRef\]](#)
66. De Lauro, E.; Petrosino, S.; Ricco, C.; Aquino, I.; Falanga, M. Medium and long period ground oscillatory pattern inferred by borehole tiltmetric data: New perspectives for the Campi Flegrei caldera crustal dynamics. *Earth Planet. Sci. Lett.* **2018**, *504*, 21–29. [\[CrossRef\]](#)
67. Spiridonov, E.A. ATLANTIDA 3. 1. Software for analysis of earth tides data. *Nauka Tekhnol. Razrab.* **2014**, *93*, 3–48.
68. Kumpel, H.-J.; Lehmann, K.; Fabian, M.; Montes, G.Y. Point stability at shallow depths: Experience from tilt measurements in the Lower Rhine Embayment, Germany, and implications for high-resolution GPS and gravity recordings. *Geophys. J. Int.* **2001**, *146*, 699–713.
69. Fabian, M.; Kumpel, H.-J. Poroelasticity. Observations of anomalous near surface tilt induced by ground water pumping. *J. Hydrol.* **2003**, *281*, 187. [\[CrossRef\]](#)
70. Fabian, M. Near surface tilt and pore pressure changes induced by pumping in multi-layered poroelastic half-spaces. Ph.D. Thesis, Berichte aus der Geowissenschaft, Universitaet Bremen, Bremen, Germany, 2004; p. 121.
71. Queitsch, M.; Jentzsch, G.; Weise, A.; Ishii, H.; Asai, Y. Pumping induced pore pressure changes in tilt measurements near a fault zone in Mizunami, Japan. In *Proceedings of the International Association of Geodesy Symposia*; Springer: Berlin, Germany, 2014; Volume 139, pp. 113–118.
72. Savage, M.K.; Ferrazzini, V.; Peltier, A.; Rivemale, E.; Mayor, J.; Schmid, A.; Brenguier, F.; Massin, F.; Got, J.-L.; Battaglia, J.; et al. Seismic anisotropy and its precursory change before eruptions at Piton de la Fournaise volcano. La Réunion. *J. Geophys. Res. Solid Earth.* **2015**, *120*, 3430–3458. [\[CrossRef\]](#)
73. Hainzl, S.; Ben-Zion, Y.; Cattania, C.; Wassermann, J. Testing atmospheric and tidal earthquake triggering at Mt. Hochstaufen, Germany. *J. Geophys. Res. Solid Earth.* **2013**, *118*, 5442–5452. [\[CrossRef\]](#)

74. Farquharson, J.I.; Wadsworth, F.B.; Heap, M.J.; Baud, P. Time-dependent permeability evolution in compacting volcanic fracture systems and implications for gas overpressure. *J. Volcanol. Geotherm. Res.* **2017**, *339*, 81–97. [[CrossRef](#)]
75. Girona, T.; Huber, C.; Caudron, C. Sensitivity to lunar cycles prior to the 2007 eruption of Ruapehu volcano. *Sci. Rep.* **2018**, *8*, 1476. [[CrossRef](#)] [[PubMed](#)]
76. Albino, F.; Amelung, F.; Gregg, P. The role of pore fluid pressure on the failure of magma reservoirs: Insights from Indonesian and Aleutian arc volcanoes. *J. Geophys. Res. Solid Earth.* **2018**, *123*, 1328–1349. [[CrossRef](#)]
77. Juncu, D.; Árnadóttir, T.; Geirsson, H.; Guðmundsson, G.B.; Lund, B.; Gunnarsson, G.; Hoopere, A.; Hreinsdóttir, S.; Michalczevska, K. Injection-induced surface deformation and seismicity at the Hellisheidi geothermal field, Iceland. *J. Volcanol. Geotherm. Res.* **2018**, in press. [[CrossRef](#)]
78. Piochi, M.; Kilburn, C.R.J.; Di Vito, M.A.; Mormone, A.; Tramelli, A.; Troise, C.; De Natale, G. The volcanic and geothermally active Campi Flegrei caldera: An integrated multidisciplinary image of its buried structure. *Int. J. Earth Sci.* **2014**, *103*, 401–421. [[CrossRef](#)]
79. De Lauro, E.; De Martino, S.; Falanga, M.; Petrosino, S. Synchronization between tides and sustained oscillations of the hydrothermal system of Campi Flegrei (Italy). *Geochem. Geophys. Geosyst.* **2013**, *14*, 2628–2637. [[CrossRef](#)]
80. Chiodini, G.; Selva, J.; Del Pezzo, E.; Marsan, D.; De Siena, L.; D’Auria, L.; Bianco, F.; Caliro, S.; De Martino, P.; Ricciolino, P.; et al. Clues on the origin of post-2000 earthquakes at Campi Flegrei caldera (Italy). *Sci. Rep.* **2017**, *7*, 4472. [[CrossRef](#)]



© 2019 by the authors. Licensee MDPI, Basel, Switzerland. This article is an open access article distributed under the terms and conditions of the Creative Commons Attribution (CC BY) license (<http://creativecommons.org/licenses/by/4.0/>).